Quantum Modeling of Thermoelectric Properties of Si/Ge/Si Superlattices

Anuradha Bulusu and D. Greg Walker

***Abstract*—Using a nonequilibrium Green's function approach, quantum simulations are performed to assess the device characteristics for cross-plane transport in Si/Ge/Si-superlattice thin films. The effect of quantum confinement on the Seebeck coefficient and electrical transport and its impact on the power factor of superlattices are studied. In this case, decreasing well width leads to an increased subband spacing causing the Seebeck coefficient of the superlattice to decrease. Electron confinement also causes a drastic reduction in the overall available density of states. Results show that confinement effects in the silicon barrier are responsible for a 40% decrease in the electrical conductivity of superlattices where barrier films are thinner by a factor of 1.5. In the same two devices, there is a negligible change in the Seebeck coefficient, which results in a decrease in the power factor corresponding to the decrease in conductivity. This decrease in the electrical performance for superlattices with thinner layers may offset the previously hypothesized gains of highly scaled superlattice structures resulting from reduced thermal conductivity. Simulations of the present superlattice structure at varying doping levels show a decrease in power factor with a decrease in device size parameters.**

***Index Terms*—Nonequilibrium Green's function (NEGF), quantum confinement, thermoelectric.**

I. Introduction

THE EFFICIENCY of thermoelectric materials is usually characterized by the dimensionless thermoelectric figure of merit $\mathrm{ZT} = (S^2\sigma T)/\kappa$, where S is the Seebeck coefficient, σ is the electrical conductivity, and κ is the thermal conductivity. In the past decade, the use of confined structures such as quantum-well and quantum-wire superlattices have gained attention as thermoelectric materials due to a number of advantages: 1) the Seebeck coefficient can be increased by the increase in the local density of density of states per unit volume near the Fermi energy [1]; and 2) the thermal conductivity can be decreased due to phonon confinement [2], [3] and phonon scattering at the material interfaces in the superlattice [4]–[6]. Normally, the electrical conductivity is assumed not to be significantly affected due to the large semiconductor bandgap and the disparity between the electron and phonon mean free paths [7]. The combined benefits of a reduced thermal conductivity and an improved Seebeck coefficient imply a theoretically higher ZT compared to the bulk structures. However, experimental observations, particularly in the case of Si/Ge superlattices, have not been able to achieve the presumed benefits of superlattice thermoelectric devices despite the theoretically predicted improvements in ZT and the experimentally observed reduction in the thermal conductivity of the superlattices compared to their bulk counterparts [1], [8]. Hence, there is a need to better understand the effect of all the significant factors contributing to the thermoelectric figure of merit of nanoscale devices including the electrical conductivity σ.

The dominant reduction in thermal conductivity in the superlattices is in the cross-plane direction [9]–[11]. However, thermoelectric performance in the in-plane direction has been studied extensively mainly due to the difficulty associated with conducting experiments in the cross-plane direction because of the very small film thicknesses and the effect of the large contact resistances [12], [13]. Interest in in-plane transport is also motivated by the higher mobility of electrons due to substrate strain [8], [14]. Yang *et al.* [12] measured the anisotropic behavior of in-plane and cross-plane superlattices and found that while the Seebeck coefficient did not change significantly, the electrical conductivity, as well as thermal conductivity in the cross-plane direction, is five to six times lower than the in-plane direction. The study of cross-plane transport in this paper is motivated by the higher decrease in thermal conductivity, as well as the opportunity to study and to understand quantum effects with a view to tune the electrical performance of superlattices by changing various parameters, such as the thickness of layers, doping, etc.

Experimental data of quantum effects on electrical conductivity is limited. However, the effect of confinement on electron mobility has been widely studied [15], [16]. It was found that intersubband scattering increased when the subband energy spacing for electrons was less than twice the polar optical phonon energy [17], leading to a reduced electron mobility in confined structures. However, recent theoretical studies of nanowires coated with an acoustically hard barrier shell [18] have predicted an enhanced mobility of nanowires. The effects of confinement on the figure of merit have been studied as a function of the superlattice period in [19] using a constant-relaxation-time-approximation (RTA) model with a Kronig–Penny dispersion relation. Based on their calculations, the value of ZT reached a maximum limit as a function of the quantum-well width. They theorized that for small barrier widths, electron tunneling caused the value of ZT to decrease, whereas for large barrier widths, the parasitic effect of backflow of heat from the barriers resulted in the low ZT values. It is

Manuscript received April 2, 2007; revised June 26, 2007. This work was supported in part by the National Science Foundation under Grant 0554089 and by a Vanderbilt Discovery grant. The review of this paper was arranged by Editor S. Datta.

The authors are with the Department of Mechanical Engineering, Vanderbilt University, Nashville, TN 37235 USA (e-mail: greg.walker@vanderbilt.edu).

Color versions of one or more of the figures in this paper are available online at http://ieeexplore.ieee.org.

Digital Object Identifier 10.1109/TED.2007.910574

clear from all the above studies that isolating and understanding the impact of quantum effects on the electrical conductivity and Seebeck coefficient are critical for the development of thermoelectric structures.

The most common method of predicting thermoelectric parameters is based on a semiclassical RTA model [1], [4]–[6] where the system is assumed to be only slightly perturbed from equilibrium. Some of the early models employed parabolic energy dispersion for the conduction and valance band energies, whereas later models incorporated the effect of low dimensionality through a subband energy-dispersion relation [1], [4], [5], [8]. Although these models use confined dispersion relations, transport and thermoelectric coefficients are still calculated using the semiclassical RTA model that cannot adequately capture wave effects. Quantum effects such as tunneling are usually introduced in semiclassical models using correction terms [20], [21]. On the other hand, purely quantum-transport models [22], [23] that involve the solution to the Schrödinger equation are limited to studying the current flow where transport is generally ballistic or includes very limited scattering. In this regard, the nonequilibrium Green's function (NEGF) formalism provides a framework for coupling quantum effects and thermal effects to model the electron transport in thermoelectric devices. Open boundary conditions allow the source and drain contacts to be coupled to the device through simple self-energy terms that eliminate the need for huge matrices that are of the size of the source- and drain-reservoir systems. Instead, matrices in the NEGF formalism are the size of the device Hamiltonian. In addition, the NEGF formalism does not require a statistical distribution of carriers within the device thus allowing for the rigorous incorporation of both elastic and inelastic scattering effects using the concept of Buttiker probes [24]. A brief synopsis of the formalism is provided in the next section, whereas a more thorough and detailed development can be found in [25].

In this work, the Green's function approach is used to study the impact of electron confinement on the cross-plane thermoelectric properties of Si/Ge/Si quantum-well superlattices with varying film thicknesses. As such, the electron transport is modeled as purely ballistic, neglecting the scattering effects. We realize that additional effects such as electron–phonon scattering may influence the overall thermoelectric performance. The impact of electron–phonon scattering on thermoelectric properties have been studied using the NEGF method and can be found in our works [26], [27]. In those works, electrons in strained superlattices with structures similar to those studied in this paper are modeled to undergo both the elastic and inelastic scattering with phonons. For the size of the superlattices considered, the Seebeck coefficient does not change, whereas the electrical conductivity showed a 43%–64% decrease when electrons scatter with optical phonons. While incorporation of scattering effects is important to obtain a comprehensive prediction of the thermoelectric performance of nanostructures, the motivation of this paper is to model, to isolate, and to understand the quantum effects on the thermoelectric performance of nanostructured materials. As such, the assumption of ballistic transport does not limit the generality of the study of quantum confinement and tunneling on the thermoelectric behavior in these devices.

II. NEGF Formalism

Consider the case of an open system consisting of a channel connected to the source and drain contacts. Let μ_1 and μ_2 be the chemical potentials of the source and the drain. The distribution of electrons in the semi-infinite source and the drain is said to follow the Fermi distribution. For a 2-D film, the Fermi function is given by considering the electrons to have periodic boundaries in the infinite x- and y-directions and to experience confinement along the z-direction

$$f_{2\mathrm{D}} = N_0 \ln\left(1+\exp\left(\frac{-E}{k_BT}\right)\right), \text{ where } N_0 = \frac{m_c k_B T}{2\pi\hbar^2}. \tag{1}$$

In the NEGF formalism, the coupling of the device to the source and drain contacts is described using self-energy matrices $\sum_1$ and $\sum_2$. The self-energy term can be viewed as a modification to the channel Hamiltonian to incorporate the boundary conditions and can be written as

$$(H+U+\Sigma_1+\Sigma_2)\psi_\alpha(\vec{r}) = \varepsilon_\alpha\psi_\alpha(\vec{r}). \tag{2}$$

The self-energy term $\sum$ originates from the solution of the contact Hamiltonian. In this semi-infinite system, which is connected to the channel, there will be an incident wave from the channel, as well as a reflected wave from the contact. Whereas the incoming electron from the contact will have infinite wave vectors in all the three directions, the channel wave vector along the z-axis will occupy only discrete finite energy levels due to the formation of energy subbands along the z-direction. The wave function at the interface is matched to conserve energy. The energy-conservation equation can be written as shown in

$$E(k) = E_c + \frac{\hbar^2k_x^2}{2m_x^*} + \frac{\hbar^2k_y^2}{2m_y^*} + \frac{\hbar^2}{2m_z^*}\left(\frac{n\pi}{L_z}\right)^2, \quad \text{where } n = 1,2,3,\ldots. \tag{3}$$

The term $k_z = n\pi/L_z$ is the wave vector corresponding to the confined electrons that form discrete standing waves when confined in an infinite potential well.

The superlattice considered in this paper is modeled as a 1-D grid with a spacing of a and the number of grid points N, such that the silicon-film thickness is given by $L_{\mathrm{Si}} = a(N_{\mathrm{Si}}-1)$. The thickness of germanium film is $L_{\mathrm{Ge}} = a(N_{\mathrm{Ge}}-1)$. As the thickness of each layer changes, the grid spacing is determined to ensure that the value of t (5) is always greater than the energy range of integration above the conduction band [25]. The electron transport is modeled in the cross-plane direction of the superlattice, which is also the confined direction. We use an effective mass Hamiltonian. The integration range for electron energy is from -1 to 1 eV for over 1200 integration steps. The integration step size and lattice spacing were adjusted to ensure that convergence and grid independence were obtained.

The incoming wave vectors along the transverse x- and y-axes are taken to be equal to k, resulting in the boundary condition

$$\Sigma_i = -t\exp(ika) \tag{4}$$

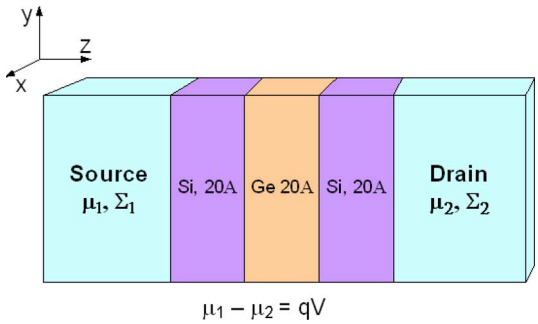

Fig. 1. Schematic representation of a Si/Ge/Si quantum-well superlattice modeled in the simulation.

where t, the interunit coupling energy resulting from the discretization, is given by

$$t = \frac{\hbar^2}{2m^* a^2}. \tag{5}$$

The source and drain self-energy terms are combined in the device Hamiltonian (2) to solve for the energy eigenvalues in the channel from which the channel current is obtained. The entire calculation is carried out self-consistently with Poisson's equation to account for the change in channel potential with the change in electron density. The doping for each film in the superlattice is applied by changing the relative energy between the Fermi level and the conduction-band edge for each material using the relation [28]

$$n = N_c \exp\left(-\frac{(E_c - E_f)}{k_B T}\right). \tag{6}$$

III. Results

The device under study consists of a single quantum well formed by alternating layers of silicon, germanium, and silicon thin films, as shown in Fig. 1, with transport in the cross-plane direction. Electron confinement in the device occurs for two reasons. 1) The very small thickness of the films gives rise to discretely spaced energy subbands in the cross-plane z-direction. 2) For the constant doping levels in all the three layers, the larger bandgap of the silicon layers on either side of the germanium layer sets up a potential barrier for the electrons in germanium thus causing an additional confinement of the electrons in germanium leading to a 1-D potential well. The electron transport in the device under an applied bias is modeled along the confined z-direction, and the current is calculated for over ten subbands. The Seebeck coefficient for the well was studied for various temperature ranges of the source and drain contacts while varying the doping in the Si/Ge/Si well. The source temperature was maintained constant at 300 K while the drain contact was maintained at a higher temperature relative to the source. The applied bias ranged from 0 to 0.1 V.

Fig. 2 shows the cross-plane current–voltage characteristics for a ballistic Si(20 Å)/Ge(20 Å)/Si(20 Å) quantum well doped to a concentration of 5×10^{18} cm^{-3}. The source–drain temperature difference ranges from 0 K to a maximum of 30 K. The higher temperature at the drain results in the diffusion of electrons from the drain toward the source, opposing the direction of the bias leading to negative current values. As the applied bias is increased, more electrons from the source drift toward the drain, and at a particular voltage, which we call the Seebeck voltage, the diffusion of electrons from the drain to the source is balanced by the drift current from the source to the drain leading to zero current. The Seebeck voltage obtained for each temperature gradient is divided by that value of the gradient to obtain the Seebeck coefficient.

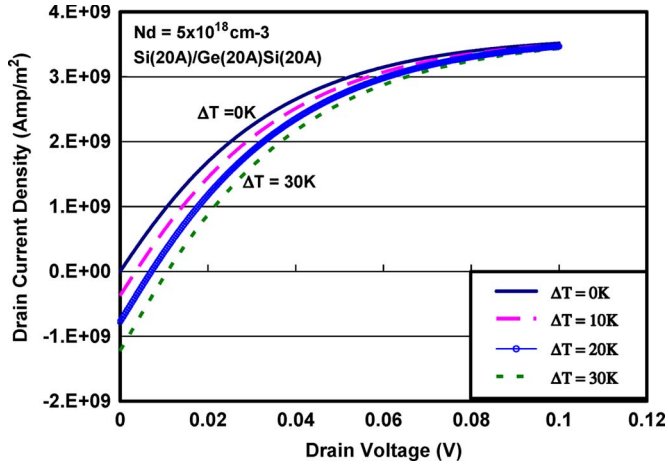

Fig. 2. Current density–voltage characteristics of a ballistic Si(20 Å)/Ge(20 Å)/Si(20 Å) quantum-well structure. Channel-temperature difference ranges from 0 to 30 K.

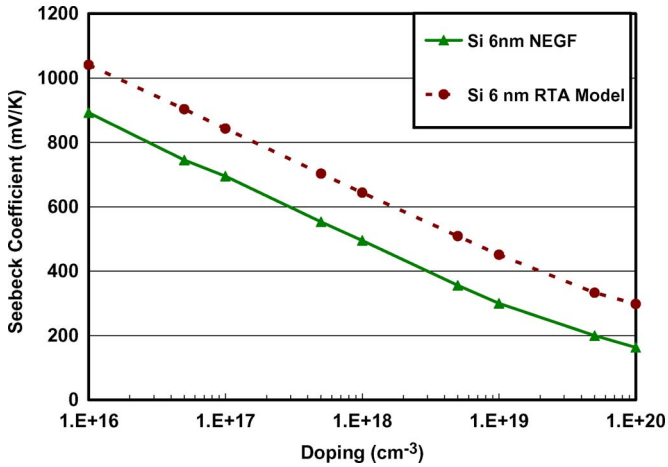

Fig. 3. Seebeck coefficient versus doping for silicon films using the NEGF and an RTA model.

Fig. 3 shows the Seebeck coefficient of 6-nm-thick silicon films predicted using the NEGF model compared to the values obtained from an RTA model [4] using a confined dispersion for electron confinement in the z-direction. Whereas we do not expect an exact match due to the very different nature of the two models, the Seebeck-coefficient values from the NEGF model follow a similar trend as the RTA model.

Fig. 4 shows the electrical-conductivity values as a function of doping for the 6-nm silicon film obtained from the NEGF and RTA models. The doping in both models is applied using (6) by varying the relative difference between the Fermi level and conduction-band edge. In addition, the RTA model requires the value of mobility in the direction of transport for electrical-conductivity calculations. Because of the conflict

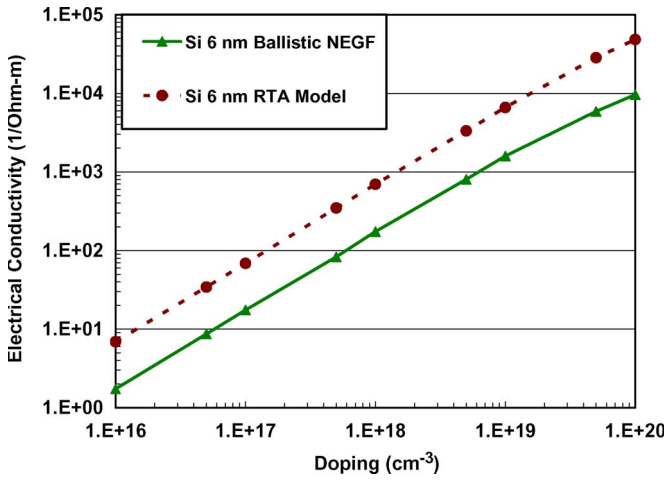

Fig. 4. Electrical conductivity versus doping for silicon films using the NEGF and RTA models.

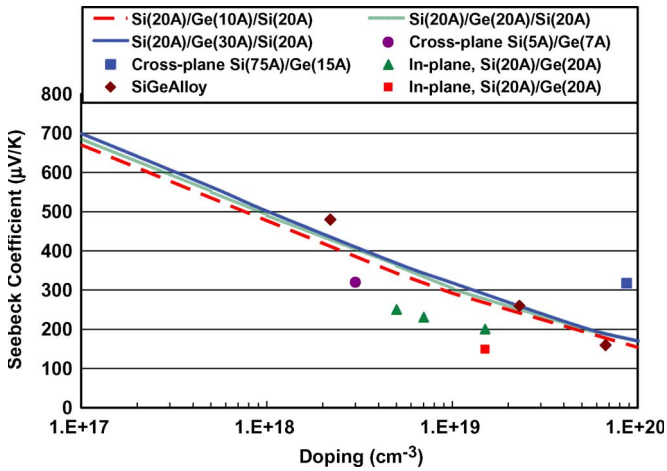

Fig. 5. Seebeck coefficient versus doping for Si/Ge/Si superlattices for various thicknesses. Experimental data taken from [8] and [30]–[33].

in the electron-mobility behavior with the decreasing film thickness seen in the literature [15]–[18], we use the bulk mobility value of silicon as a benchmark for calculating the electrical conductivity using the RTA model. Despite the NEGF model which is treating the electron transport as ballistic, the conductivity values predicted by the NEGF method are lower than the predictions of the RTA model. The lower conductivity values are attributed to the limited number of electron-energy levels available for the conduction in the 6-nm film due to the confinement effects that are captured by the NEGF model. These results support our hypothesis that confinement effects dominate at these size regimes.

Fig. 5 shows the cross-plane Seebeck-coefficient values as a function of the doping levels for the Si/Ge/Si quantum-well superlattices. The predicted Seebeck coefficient for each doping is an average of the value obtained for each temperature gradient. The results from our simulations are compared to the measured values found in the literature. Considering the large spread in the experimentally measured values of the Seebeck coefficient for various doping levels, our results are in fair agreement with the measured values. In addition, the trend predicted by the NEGF model matches the experimental data where an increase

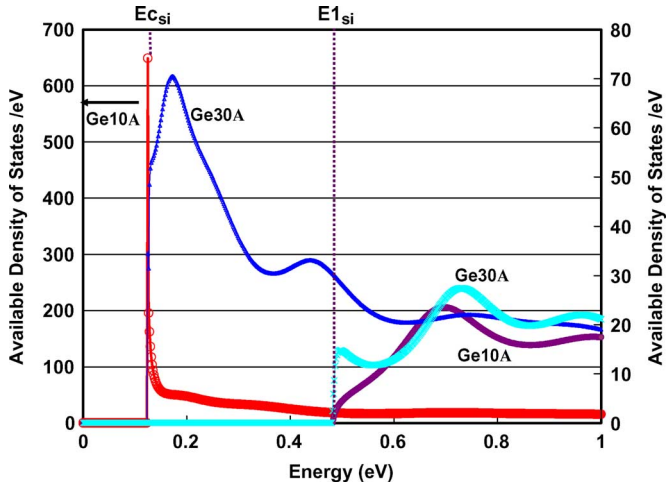

Fig. 6. Available density of states distribution versus energy for Si(20 Å)/Ge(10 Å)/Si(20 Å) and Si(20 Å)/Ge(30 Å)/Si(20 Å) superlattices. Ec_{si} and $E1_{si}$ represent the conduction band and the first subband energies in silicon, respectively. All curves are plotted against the right axis except where noted.

in doping leads to a reduced Seebeck coefficient. We do not expect our data to exactly match experimental measurements for a number of reasons that will be discussed later.

The NEGF method was used to compare the change in the Seebeck coefficient due to the confinement. For a constant silicon-barrier thickness of 20 A, we compare the Seebeck coefficients by varying the germanium-well thickness from 10 to 20 Å and 30 Å. It is shown Fig. 5 that the calculated Seebeck-coefficient values show a gradual increase in the Seebeck coefficient between the 10- and 20-Å and 30-Å well sizes for a given doping level such that the difference in the Seebeck coefficients between Ge 10-Å well and Ge 30-Å well is approximately 30 μV/K. The reason for the change in the Seebeck coefficient can be understood by looking at the distribution for the available density of states per unit energy of the 10- and 30-Å wells shown in Fig. 6. In our simulations, the major contribution to the current comes from the conduction band and the first subband. Since electrons from the contacts enter through silicon, the conduction-band edge and the first subband energies for silicon are also shown here by the dotted lines for reference purposes. To understand the theory behind the physics of the Seebeck coefficient, consider the case of the Ge 10-Å well. The density of states for the conduction band Ec has a value of 650 eV^{-1}, which is much higher than the value of 3 eV^{-1} near the first subband E1. When the temperature at the drain is raised, the large number of electrons near the conduction-band edge gain thermal energy and try to occupy higher energy levels. However, as the available density of states for E1 is much smaller than the states near Ec, very few electrons from the conduction band can occupy the states near the first subband E1. These drain electrons then diffuse to the silicon on the cold side filling its first subband. The drain electrons arriving at the source at energy E1 attempt to lose their thermal energy and to fall to the next lower energy corresponding to Ec. However, because most of the states near the conduction band at the source are already occupied, the hot electrons from the drain remain at the first subband energy E1

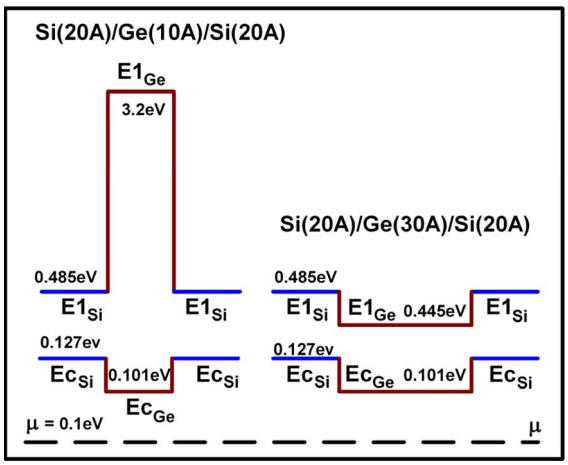

Fig. 7. Band diagram for Si(20 Å)/Ge(10 Å)/Si(20 Å) and Si(20 Å)/Ge(30 Å)/Si(20 Å) superlattices showing the conduction band and the first subband energies.

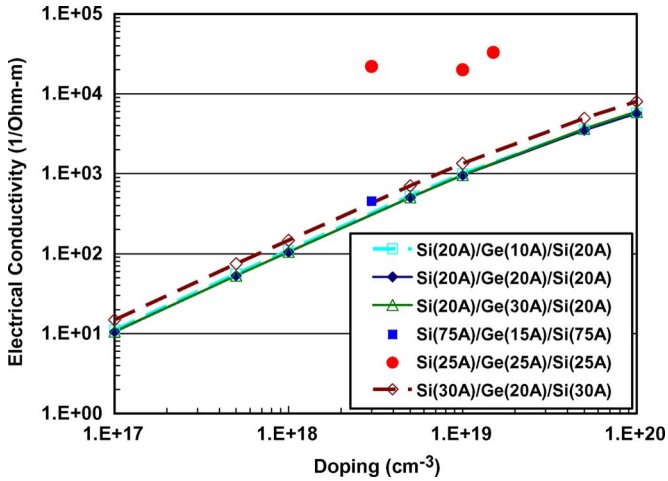

Fig. 8. Electrical conductivity versus doping for Si/Ge/Si superlattices for varying film thicknesses. Experimental data (in filled circles and square) taken from [31] and [34].

preventing additional drain electrons from diffusing toward the source, producing a voltage in the process.

While the Seebeck voltage is formed by a similar process in the Ge 30-Å case, the density of states at E1 is five times greater compared to the Ge 10-Å well. The larger density of states can be attributed to the fact that the subband spacing in the Ge 10-Å film is greater than that of the Si 20-Å film due to the confinement effects of the thinner germanium film, as shown in Fig. 7. As a result, for the energy levels around E1, there will be very little contribution from the germanium film for the electron transport. In the case of the Ge 30-Å superlattice, the subbands are more closely spaced leading to a greater contribution to transport, and hence, higher density of states around E1. While quantum confinement is commonly believed to increase the Seebeck coefficient due to the increased density of states near the Fermi energy, this difference in the density of states near E1 between the two wells is the reason that the Seebeck voltage is higher for the Si(20 Å)/Ge(30 Å)/Si(20 Å) structure compared to the Si(20 Å)/Ge(10 Å)/Si(20 Å) structure. The confinement effects were also studied for the case where the germanium-well thickness was kept constant while the silicon-barrier thickness was changed from 20 to 30 Å. In this case, the Seebeck coefficient was found not to be significantly affected by the change in the barrier thickness. This behavior can be attributed to the fact that while the silicon-barrier layers next to the source determine the supply of electrons into the superlattice, their diffusion and drift through the superlattice is governed by the density of states in the germanium well whose thickness is held constant in this case. Hence, we see no change in the Seebeck coefficient with the change in the barrier thickness.

The electrical conductivity in the cross-plane direction of the superlattice films is calculated using the slope of the linear portion of the current density–voltage curve at 300 K (shown in Fig. 2). Fig. 8 shows the change in electrical conductivity of the various superlattices with doping. For a constant silicon-barrier thickness, the electrical conductivity for the superlattice films does not vary significantly with the change in the well thickness. The reason for this behavior is that the supply of electrons is governed by the silicon-film thickness. If the germanium well is very thin, electrons can tunnel through germanium into the silicon film on the other side of the well, whereas for large well thicknesses, there will be sufficient density of states available in the germanium layer to contribute to the electron transport. In addition, the increase in doping also lowers the conduction band and subband energies, providing more states for the electron transport. The combination of quantum effects and doping resulted in a change of less than 5% in the electrical conductivity as a function of doping. However, for a constant germanium-well thickness of 20 Å when the silicon-barrier-film thickness is increased from 20 to 30 Å, the electrical conductivity of the Si(30 Å)/Ge(20 Å)/Si(30 Å) structure increases by 40% compared to the Si(20 Å)/Ge(20 Å)/Si(20 Å) superlattice. The increase in the conductivity with the increase in barrier thickness is attributed to the closer subband spacing of the 30-Å silicon film compared to the 20-Å film resulting in an increase in the density of states available for conducting electrons from the source.

The power factor $S^2\sigma$ was calculated using the electrical-conductivity values and the Seebeck coefficient obtained for each doping level that was considered. Fig. 9 shows the power-factor values for each doping level as a function of the germanium-well and silicon-barrier-film thicknesses. For the constant silicon-barrier thickness of 20 Å, the increase in the germanium-well thickness from 10 to 30 Å results in the lowering of subband energies which results in a 6% increase in the Seebeck coefficient while the electrical conductivity shows a slight change. Accordingly, as shown from Figs. 5 and 8, the slight increase in the Seebeck coefficient and the electrical conductivity for the Ge 30-Å well case translates into a 12% increase in its power factor. Similarly, for the constant germanium-well thickness of 20 Å, the thicker silicon 30-Å barrier in the Si(30 Å)/Ge(20 Å)/Si(30 Å) superlattice offers lower subband energies for the electron transport from the source compared to the 20-Å silicon-barrier layer in the Si(20 Å)/Ge(20 Å)/Si(20 Å) superlattice, leading to a 40% increase in electrical conductivity. In this case, the Seebeck coefficient showed only a very small change due to the constant well

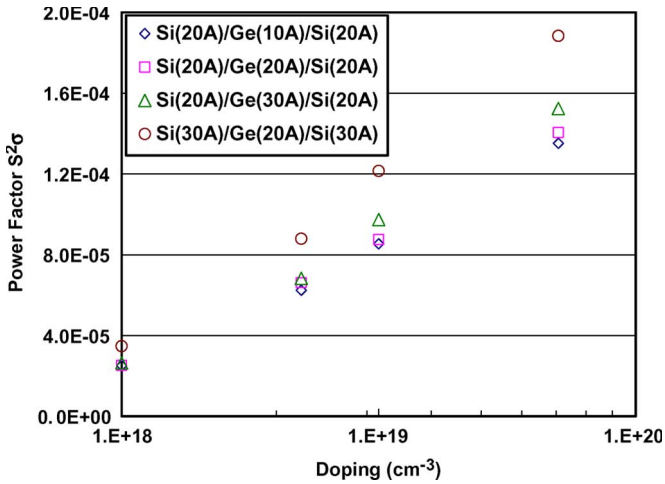

Fig. 9. Power factor versus doping for superlattices with varying film thicknesses.

thickness. The higher conductivity of the Si(30 Å)/Ge(20 Å)/Si(30 Å) superlattice dominates the power factor, resulting in a 36% increase in the power factor of this superlattice compared to the Si(20 Å)/Ge(20 Å)/Si(20 Å) superlattice.

In addition to the effects of quantum confinement, the values used for the effective mass for silicon and germanium were found to have a significant effect on the predicted electrical-conductivity values. For our calculations, we used the effective mass corresponding to bulk conductivity values, but the various experiments in [8], [30], [31], and [33] were performed on single crystalline epitaxial layers deposited on a graded Si_xGe_{1-x} substrate. For film thicknesses of the order of a few nanometers, as used in our calculations, both silicon and germanium can be considered to be single crystals, allowing us to use the effective mass for that particular orientation. In addition, the graded substrate used in the experiments introduces lateral strains in the silicon and germanium films causing changes in the band structure and the formation of barriers in the germanium film [1], [14]. While these effects are important and may affect the thermoelectric properties of the superlattice, this study is relegated to another effort [27]. The results obtained in this paper are significant in that they 1) demonstrate the capability of the NEGF method to model the thermoelectric properties of quantum-well-superlattice structures and 2) allow us to isolate and study the quantum effects on the thermoelectric performance of superlattices.

IV. Conclusion

The NEGF method was used to successfully isolate and to study the quantum-confinement effects on the cross-plane thermoelectric properties of a single period Si/Ge/Si quantum-well superlattice. Confinement effects are captured in the form of an increased subband spacing and a reduction in density of states available for the electron transport between the superlattice layers. The net result is a decrease in the Seebeck coefficient of the superlattice, as well as a decreased electrical conductivity with confinement despite the ballistic nature of the electron transport. This trend may explain why measured values of ZT have not been able to corroborate other theoretical predictions of improved performance from devices with the reduced sizes. Our quantum-transport model has shown that there exists optimal values of well and barrier thicknesses below which the confinement can prove to be detrimental to the thermoelectric performance. These findings imply that the superlattice size parameters can be tuned to enhance the thermoelectric performance. The results of the device studied may not be directly generalizable to any superlattice structure and/or material because strain, band gap size, transport direction, and effective mass, for example, will affect the magnitude and onset of the confinement effects. Yet, we expect the physical response due to confinement (increased subband spacing, tunneling probability, etc.) to be similar enough in other materials that show a decrease in performance with reduced layer size. Finally, even though a single property cannot be considered in isolation for optimal performance, overall, the capability of the NEGF method as a platform to design structures with an enhanced figure of merit has been established.

Acknowledgment

The authors would like to thank Prof. S. Datta from the Department of Electrical and Computer Engineering, Purdue University for providing the manuscript of his work.

References

[1] M. S. Dresselhaus, Y. M. Lin, T. Koga, S. B. Cronin, O. Rabin, M. R. Black, and G. Dresselhaus, "Quantum wells and quantum wires for potential thermoelectric applications," in *Recent Trends in Thermoelectric Materials Research III*, vol. 71, T. M. Tritt, Ed. New York: Academic Press, 2001.

[2] A. Balandin and K. L. Wang, "Significant decrease of the lattice thermal conductivity due to phonon confinement in a free-standing semiconductor quantum well," *Phys. Rev. B, Condens. Matter*, vol. 58, no. 3, pp. 1544–1549, Jul. 1998.

[3] A. Balandin and K. L. Wang, "Effect of phonon confinement on the thermoelectric figure of merit of quantum wells," *J. Appl. Phys.*, vol. 84, no. 11, pp. 6149–6153, Dec. 1998.

[4] L. D. Hicks and M. S. Dresselhaus, "Effect of quantum well structures on the thermoelectric figure of merit," *Phys. Rev. B, Condens. Matter*, vol. 47, no. 19, pp. 12 727–12 731, May 1993.

[5] L. D. Hicks, T. C. Harman, and M. S. Dresselhaus, "Use of quantum-well superlattices to obtain a high figure of merit from nonconventional thermoelectric materials," *Appl. Phys. Lett.*, vol. 63, no. 23, pp. 3230–3232, Dec. 1993.

[6] L. W. Whitlow and T. Hirano, "Superlattice applications to thermoelectricity," *J. Appl. Phys.*, vol. 78, no. 9, pp. 5460–5466, Nov. 1995.

[7] M. S. Dresselhaus, "Nanostructures and energy conversion," in *Proc. Rohsenhow Symp. Future Trends Heat Transfer*, Cambridge, MA, May 16, 2003.

[8] T. Koga, S. B. Cronin, M. S. Dresselhaus, J. L. Liu, and K. L. Wang, "Experimental proof-of-principle investigation of enhanced $Z_{3D}T$ in 001 oriented Si/Ge superlattices," *Appl. Phys. Lett.*, vol. 77, no. 10, pp. 1–3, Sep. 2000.

[9] G. Chen, C. L. Tien, X. Wu, and J. S. Smith, "Thermal diffusivity measurement of GaAs/AlGaAs thin-film structures," *Trans. ASME, J. Heat Transf.*, vol. 116, no. 2, pp. 325–334, May 1994.

[10] W. S. Capinski and H. J. Maris, "Thermal conductivity of GaAs/AlAs superlattices," *Phys. Rev. B, Condens. Matter*, vol. 219/220, pp. 699–701, 1996.

[11] S. M. Lee, D. G. Cahill, and R. Venkatasubramanian, "Thermal conductivity of Si–Ge superlattices," *Appl. Phys. Lett.*, vol. 70, no. 22, pp. 2957–2959, Jun. 1997.

[12] B. Yang, W. L. Liu, J. L. Liu, K. L. Wang, and G. Chen, "Measurements of anisotropic thermoelectric properties in superlattices," *Appl. Phys. Lett.*, vol. 81, no. 19, pp. 3588–3590, Nov. 2002.

[13] R. Venkatasubramanian, E. Sivola, T. Colpitts, and B. O'Quinn, "Thin-film thermoelectric devices with high room-temperature figures of merit," *Nature*, vol. 413, no. 6856, pp. 597–602, Oct. 2001.
[14] C. G. Vand de Walle, "Band lineups and deformation potentials in the model-solid theory," *Phys. Rev. B, Condens. Matter*, vol. 39, no. 3, pp. 1871–1883, Jan. 1989.
[15] J. H. Choi, Y. J. Park, and H. S. Min, "Electron mobility behavior in extremely thin SOI MOSFETs," *IEEE Electron Device Lett.*, vol. 16, no. 11, pp. 527–529, Nov. 1995.
[16] S. Takagi, J. Koga, and A. Toriumi, "Subband structure engineering for performance enhancement of Si MOSFETs," in *IEDM Tech. Dig.*, 1997, pp. 219–222.
[17] T. Wang, T. H. Hsieh, and T. W. Chen, "Quantum confinement effects on low-dimensional electron mobility," *J. Appl. Phys.*, vol. 74, no. 1, pp. 426–430, Jul. 1993.
[18] V. A. Fonoberov and A. A. Balandin, "Giant enhancement of the carrier mobility in silicon nanowires with diamond coating," *Nano Lett.*, vol. 6, no. 11, pp. 2442–2446, 2006.
[19] J. O. Sofo and G. D. Mahan, "Thermoelectric figure of merit of superlattices," *Appl. Phys. Lett.*, vol. 65, no. 21, pp. 2690–2692, Nov. 1994.
[20] A. Asenov, J. R. Watling, A. R. Brown, and D. K. Ferry, "The use of quantum potentials for confinement and tunnelling in semiconductor devices," *J. Comput. Electron.*, vol. 1, no. 4, pp. 503–513, Dec. 2002.
[21] T. W. Tang and B. Wu, "Quantum correction for the Monte Carlo simulation via the effective conduction-band edge equation," *Semicond. Sci. Technol.*, vol. 19, no. 1, pp. 54–60, Jan. 2004.
[22] C. S. Lent and D. J. Kirkner, "The quantum transmitting boundary method," *J. Appl. Phys.*, vol. 67, no. 10, pp. 6353–6359, May 1990.
[23] S. E. Laux, A. Kumar, and M. V. Fischetti, "Ballistic FET modeling using QDAME: Quantum device analysis by modal evaluation," *IEEE Trans. Nanotechnol.*, vol. 1, no. 4, pp. 255–259, Dec. 2002.
[24] S. Datta, "Nanoscale device simulation: The Green's function formalism," *Superlattices Microstruct.*, vol. 28, no. 4, pp. 253–278, 2000.
[25] S. Datta, *Quantum Transport: Atom to Transistor*. New York: Cambridge Univ. Press, 2005.
[26] A. Bulusu and D. G. Walker, "Modeling of thermoelectric properties of semi-conductor thin films with quantum and scattering effects," *J. Heat Transf.*, vol. 129, no. 4, pp. 492–499, 2007.
[27] A. Bulusu, "Coupled quantum-scattering modeling of thermoelectric performance of nanostructured materials using the nonequilibrium Green's function method," Ph.D. dissertation, Vanderbilt Univ., Nashville, TN, 2007.
[28] R. Muller, T. Kamins, and M. Chan, *Device Electronics for Integrated Circuits*. New York: Wiley, 1986.
[29] K. Rim, K. Chan, L. Shi, D. Boyd, J. Ott, N. Klymko, F. Cardone, L. Tai, S. Koester, M. Cobb, D. Canaperi, B. To, E. Duch, I. Babich, R. Carmthers, P. Saunders, G. Walker, Y. Zhang, M. Steen, and M. Ieon, "Fabrication and mobility characteristics of ultra-thin strained Si directly on insulator (SSDOI) MOSFETs," in *IEDM Tech. Dig.*, 2003, pp. 49–52.
[30] B. Yang, J. L. Liu, K. L. Wang, and G. Chen, "Simultaneous measurements of Seebeck coefficient and thermal conductivity across superlattice," *Appl. Phys. Lett.*, vol. 80, no. 10, pp. 1758–1760, Mar. 2002.
[31] B. Yang, J. Liu, K. Wang, and G. Chen, "Cross-plane thermoelectric properties in Si/Ge superlattices," in *Proc. Mater. Res. Soc.*, 2002, vol. 691, pp. G.3.2.1–G.3.2.6.
[32] J. P. Dismukes, L. Ekstrom, E. F. Steigmeier, I. Kudman, and D. S. Beers, "Thermal and electrical properties of highly doped Ge–Si alloys up to 1300 °K," *J. Appl. Phys.*, vol. 10, no. 35, pp. 2899–2907, 1964.
[33] W. L. Liu, T. B. Tasciuc, J. L. Liu, K. Taka, K. L. Wang, M. S. Dresselhaus, and G. Chen, "In-plane thermoelectric properties of Si/Ge superlattice," in *Proc. Int. Conf. Thermoelectrics*, 2001, pp. 340–343.
[34] R. Venkatasubramanian, T. Colpitts, E. Watko, and D. Malta, "Experimental evidence of improved thermoelectric properties at 300 K in Si/Ge superlattice structures," in *Proc. Spring Meeting Mater. Res. Soc.*, San Francisco, CA, Mar. 31–Apr. 4, 1997.

Anuradha Bulusu received the M.S. degree in mechanical engineering from the University of Massachusetts, Lowell, and the Ph.D. degree in materials science from Vanderbilt University, Nashville, TN.

She is a Research Associate in the Department of Mechanical Engineering, Vanderbilt University. Her interests involve quantum modeling and the study of nonequilibrium electron and thermal transport in nanostructures.

D. Greg Walker received the Ph.D. degree from the Virginia Polytechnic Institute and State University, Blacksburg, in 1997, where he worked on high-speed flows and inverse heat conduction problems.

After working for a couple of years at a start-up software company that catered to the aerospace industry, he returned to academia as a Research Assistant Professor with Vanderbilt University, where he studied microscale energy transport phenomena and worked on device-level physics of microelectronic devices. Since 2001, he has been an Assistant Professor with the Department of Mechanical Engineering, Vanderbilt University, where he continues to explore energy transport and conversion in small-scale devices. His research focuses on the modeling and simulation of nonequilibrium coupled energy transport in heat-transfer and electronic materials.